Molecular Dynamics Study of Dielectric Response in a Relaxor Ferroelectric

Ilya Grinberg, Young-Han Shin, and Andrew M. Rappe
The Makineni Theoretical Laboratories, Department of Chemistry, University of Pennsylvania, Philadelphia, Pennsylvania 19104-6323, USA
(Received 8 July 2009; published 5 November 2009)

We use atomistic molecular dynamics simulations to study relaxor behavior in the $0.75PbMg_{1/3}Nb_{2/3}O_3$-$0.25PbTiO_3$ material. Even for a fairly small simulation size of 1000 atoms, the system exhibits frequency dispersion and deviation from the Curie-Weiss law typical of relaxor materials. Analysis of the time autocorrelation functions for individual atoms allows us to identify the Nb atoms with a high concentration of neighboring Ti atoms as the nucleation sites for the relaxor behavior. This is due to the higher coupling between the cation displacements induced by the presence of overbonded oxygen atoms.

DOI: 10.1103/PhysRevLett.103.197601 PACS numbers: 77.80.Bh, 77.22.−d, 77.84.−s

Since the first synthesis of the classic $PbMg_{1/3}Nb_{2/3}O_3$ (PMN) material in 1961 [1], relaxor ferroelectrics have been the subject of ongoing experimental and theoretical investigation [2–8] due to their fundamental scientific interest and their importance in technological applications such as capacitors and piezoelectric devices [9]. Relaxors exhibit a wealth of interesting physical phenomena, which first appear at the so-called Burns temperature (T_b) significantly above the Curie temperature T_c. Most prominently, below T_b, relaxor systems display a deviation of the inverse dielectric constant ($1/\epsilon$) from the Curie-Weiss law [Fig. 1(a)] [10] as well a strong dependence of the ϵ on frequency. Microscopically, modeling of the frequency dependence of ϵ has revealed a wide range of relaxation times and divergence of the longest relaxation times close to T_c [11,12].

Since the landmark paper of Burns and Dacol [13], these effects have been ascribed to the appearance of polar nanoregions (PNR) at the Burns temperature and their subsequent growth as the temperature is lowered. The PNRs are postulated to consist of groups of many correlated dipoles that move together slowly and would explain the long relaxation times that are observed [4,14]. Despite the intense research, the structure and dynamics of PNR and the relaxor phase in general on an atomistic level remain poorly understood.

In this Letter, we report that first-principles-derived atomistic simulations of $0.75PbMg_{1/3}Nb_{2/3}O_3$-$0.25PbTiO_3$ (PMN-PT) both exhibit all the dielectric signatures of relaxor behavior, and are amenable to ultrahigh resolution spatial and temporal decomposition of this relaxor response. This enables identification of an atomic-scale origin for the relaxor ferroelectric phenomenon.

We study the well-known $(1-x)$PMN-xPT material at $x = 0.25$ with full "random-site" [15] ordering to simplify the analysis of the data. Despite the B-cation ordering (rocksalt order, with only Nb on B' sites and Mg and Ti randomly populating the B'' sites), such systems exhibit relaxor behavior [15,16] due to the presence of overbonded and underbonded oxygen atoms [17]. The details of the atomistic model and the simulations are given in the supplementary online material [18].

Static bulk response.—We find that our simulations represent all of the salient features of the 0.75PMN-0.25PT dielectric response. The static dielectric constant, calculated from the fluctuations of the overall dipole of the system, shows a peak at $T_{\epsilon,\max} \approx 400$ K and a deviation from the Curie-Weiss ϵ temperature dependence at the Burns temperature $T_b \approx 500$ K [Fig. 1(a)]. Extrapolating the high-temperature inverse dielectric constant data to $1/\epsilon = 0$, we obtain a T_c of 415 K and a Curie constant $C = 1.5 \times 10^5$ K. All three transition temperatures and the Curie constant are in good agreement with the experimental values ($T_{\epsilon,\max} = 400$ K, $T_c = 440$ K, $T_b = 520$ K, $C = 1.3 \times 10^5$) obtained for 0.80PMN-0.20PT composition [19].

Frequency-dependent real bulk response.—The slowing of polarization dynamics below the Burns temperature is obvious from the inspection of the polarization time autocorrelation function $\Phi(t)$ [Fig. 1(b)]. In the paraelectric (PE) phase ($T > T_b$), $\Phi(t)$ decreases rapidly with the decay lifetime τ [20] on the order of 0.2 ps, and then oscillates with an amplitude of 0.025 and a period of less than 1 ps. Thus, in the PE phase, the system exhibits no memory. At the Burns temperature, $T = 500$ K, the amplitude and the period of $\Phi(t)$ oscillations dramatically increase to 0.07 and 3 ps, respectively. The short-time decay is also slower with $\tau = 0.28$ ps. The jump in the amplitude and period of oscillations indicates the appearance of a new, THz frequency mode, which could be narrated as the appearance of regions of slow relaxor dynamics in a paraelectric matrix. The dynamics slow down even more at $T = 400$ K with $\tau = 6.3$ ps and oscillation periods of 5 ps and 30 ps. Analysis of the short-time decay of $\Phi(t)$ allows us to estimate the freezing temperature. Plotting $1/\tau$ versus temperature and extrapolating to $1/\tau = 0$, we see that the decay time of $\Phi(t)$ becomes infinite near the freezing temperature $T_f = 380$ K [Fig. 1(b)]. This estimate of T_f

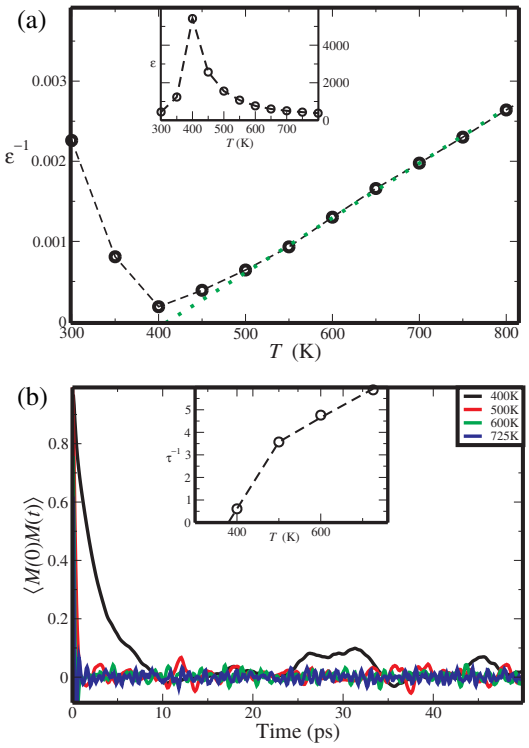

FIG. 1 (color online). (a) Inverse static dielectric constant versus temperature obtained from 0.75PMN-0.25PT MD simulations (black). Linear extrapolation of high-temperature data (dotted) allows us to estimate the T_c, which is larger than the $T_{\epsilon,\max}$. Dielectric constant dependence on temperature is shown in the inset. (b) Time autocorrelation function $\Phi(t)$ for temperatures below and above the Burns transition. Extrapolation of the short-time decay constant τ is shown in the inset.

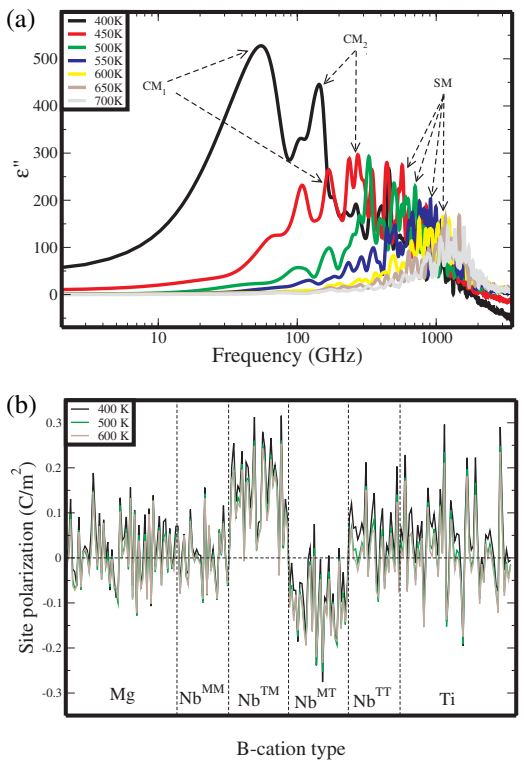

FIG. 2 (color online). (a) Dielectric loss versus frequency for series of temperatures. Below the Burns temperature, two new loss peaks rapidly move into the GHz region as the temperature is lowered. (b) Average polarization for the B-cation sites. Sites 1–54 are Mg, sites 55–82 are Nb^{MM}, sites 83–109 are Nb^{TM}, sites 110–136 are Nb^{MT}, sites 137–162 are Nb^{TT}, and sites 163–216 are Ti. Average polarizations change slightly with lower temperature.

is in good agreement with the experimentally obtained T_f of 387 K for the 0.80PMN-0.20PT system [19].

Frequency-dependent imaginary bulk response.—Using the Laplace-Fourier transform of the $\Phi(t)$, we calculate the frequency-dependent dielectric loss [Fig. 2(a)]. Because of computational cost constraints, we are only able to examine the GHz-THz region, yet even for such a relatively small window, the results presented in Fig. 2(a) agree with several important findings of the recent extensive experimental dielectric spectroscopy study of PMN relaxor performed by Bovtun *et al.* [12]. First, both our data and experiment show that at $T > T_b$ there is only one dielectric loss mode at 1–2 THz, which Bovtun *et al.* identify as the relaxor counterpart of the traditional soft mode (SM) in ferroelectrics. The frequency of this mode softens as the temperature gets lower until T_b, at which point the mode frequency starts to slowly increase. Second, for all temperatures, the contribution of this mode to the overall dielectric loss is small, between 100 and 200. Third, both experiment and this work find that at $T < T_b$, two new modes appear (called central modes in Ref. [13]) at significantly lower frequencies compared to the soft mode and making a dominant contribution to the dielectric loss. Fourth, as the temperature is lowered the lower frequency central mode (CM_1) is redshifted more rapidly then the higher frequency central mode (CM_2). These redshifts give rise to the experimentally observed trend of the dielectric loss peak shifting rapidly to lower frequencies with lower temperature. The good agreement of the dielectric response data obtained in our relatively small (2.4 nm^3) and fully random-site ordered supercell and those found experimentally suggests that the relaxor response is driven by local Å-scale phenomena without a need for nanoscale chemically ordered regions.

Time-averaged individual atom response.—We now analyze the microscopic characteristics of our system, focusing on the impact of individual B-cation pairs. The complete atomic-level knowledge of the system in our MD simulations allows us to investigate and resolve the behavior of individual atoms in order to understand the impact of heterogeneity and local variations on the dielectric response. We focus on the B-site local environment and examine its simplest possible variation—the identity of the nearest B-cation neighbors.

Along each Cartesian axis, a B cation will have two B-cation neighbors, and because of the random-site ordering, there are only six possible combinations. The Mg and Ti atoms are all completely surrounded by Nb atoms. There

are also four kinds of Nb atoms: those with two Mg neighbors (Nb^{MM}), those with two Ti neighbors (Nb^{TT}), those with Ti on the left and Mg on the right (Nb^{TM}), and those with Mg on the left and Ti on the right (Nb^{MT}). In our simulations, there are 54 Mg sites, 25 Nb^{MM} sites, 29 Nb^{TM} sites, 29 Nb^{MT} sites, 25 Nb^{TT} sites, and 54 Ti sites.

Inspection of the time-averaged local polarization data [Fig. 2(b)] elucidates the most immediate influence of the random fields. We find that Nb^{TM} and Nb^{MT}, located in an asymmetric nearest-neighbor environment, show a strong preference for positive and negative average polarization, respectively. This is in contrast to the Nb^{TT}, Mg, and Ti sites for which symmetry is only broken for the next-nearest-neighbor B cations and for which time-averaged polarization values are distributed around 0. For the Nb^{TM} and Nb^{MT} sites, the oxygen atom between Nb and Ti is overbonded, while the oxygen atom between Nb and Mg is underbonded. The Nb atom usually shifts away from the overbonded oxygen and toward the underbonded one, resulting in a strong preference for positive or negative polarization for all Nb^{TM} and Nb^{MT} sites. Such an asymmetry in the local environment creates strong random fields, present even at high temperatures $T > T_b$, as shown in Fig. 2(b).

Time-dependent individual atom response.—The local environment also plays a crucial role in the dynamics of the local dipoles, leading to the frequency-dependent dielectric response characteristic of relaxors. We find that the slowing of dynamics exhibited by the overall dipole moment is due to only a small fraction of the sites in the system. This can be seen from an examination of the time autocorrelation functions for the individual site dipole moments [$\Phi_i(t)$]. To facilitate comparison among the sites, we study the initial decay of $\Phi_i(t)$, characterizing them by their decay lifetimes τ_i [Fig. 3(a)]. A larger τ_i is a signature of stronger memory and slower relaxation dynamics. We find that it is also generally correlated with high amplitude and long period of $\Phi_i(t)$ oscillations at large t. At 725 K, well into the paraelectric phase, relaxation is fast for all sites ($\tau_i \approx 0.2$ ps), with Nb^{TT} sites displaying slightly larger τ_i values compared to the other B-cation sites. As temperature is lowered to 600 and 550 K, still in the paraelectric phase ($T > T_b$), relaxation becomes slightly slower and the contrast between Nb^{TT} and other sites becomes more pronounced. As the temperature is lowered from 550 K to the Burns temperature of 500 K, τ_i values for Nb^{TT} sites show an increase comparable to the one observed on temperature change from 600 to 550 K. However, unlike the change from 550 to 500 K, this increase is now accompanied by a large jump in τ_i values for many Ti sites, for the first time reaching τ_i values equal to those of Nb^{TT} sites. While slow dynamics are present for individual sites in the system even at $T > T_b$, these are single Nb^{TT} pointlike (0D) dipoles and do not affect each other. It is only at Burns temperature that groups of unit cells exhibit slow dynamics, giving rise to clusters or networks of slowly responding dipoles in the material.

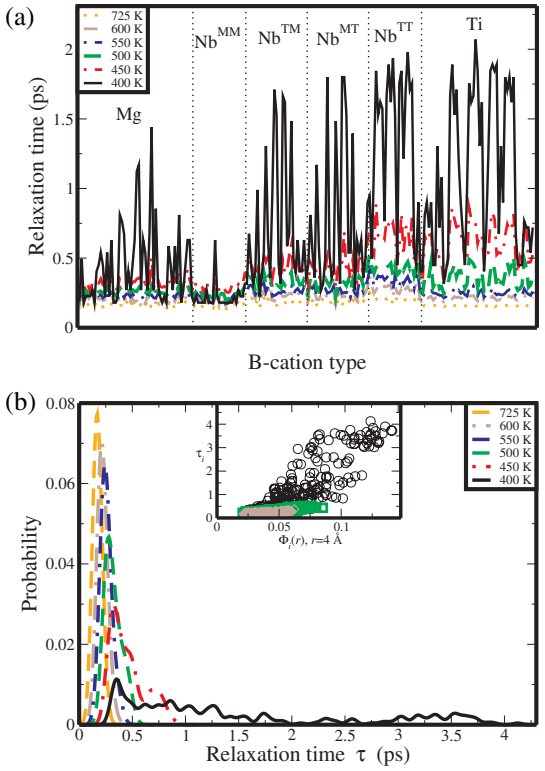

FIG. 3 (color online). (a) Relaxation time τ_i of individual B-cation sites. At T_b longer relaxation times are first exhibited not only by the Nb^{TT} sites, but also by the Ti sites, indicating the appearance of slow dynamics. (b) Distribution of the relaxation times for the B sites. The inset shows the relationship between the relaxion time τ_i and the dipole-dipole correlation function $\Phi_i(r)$ at $r = 4$ Å. High $\Phi_i(r)$ values indicate strong coupling of neighbor sites, which leads to higher τ_i.

We find that the fraction of the sites with slow dynamics grows rapidly as the temperature is lowered first to 450 K and then to 400 K. We see a rapid spread of slow relaxation first to Nb^{MT} and Nb^{TM} sites (at 450 K) and then to Mg and Nb^{MM} sites (at 400 K). However, even at the low temperatures, many sites with small τ_i ($\approx$0.5–1.0 ps) and fast dynamics are still present, indicating the relaxed crossover from fast to slow dynamics between T_b and T_f.

In agreement with phenomenological models of the experimental relaxor dielectric response data [11,12], we find that the lowering of temperature leads to a large rise in the average τ_i, a broadening of the τ_i distribution, and the divergence of the longest lifetimes [Fig. 3(b)]. In the paraelectric phase, τ_i distribution can be characterized by a narrow Gaussian distribution centered at $\approx$ 0.2–0.3 ps. At the Burns temperature of 500 K, in addition to broadening, a strong deviation from the Gaussian shape can be observed with an appearance of a shoulder at 0.5 ps. This shoulder is due to the coexistence of correlated sites, and freer dipoles. At 450 K, the distribution is clearly due to a combination of three distinct Gaussian shapes. At 400 K, the same three peaks are present. The first peak, which is due to paraelectric matrix sites, remains at a low value of

0.4 ps and does not appreciably widen compared to the τ_i distribution at $T > T_b$. The second and third peaks (roughly at 1 and 4 ps, respectively) are broad. The broadening continues on to 375 K, where some sites display τ_i values of ≈ 9 ps.

Relating ion chemistry and environment to response.—At first glance, it may be surprising that the Nb^{TT} sites which are in a symmetric environment and overall do not exhibit a preferred polarization direction, act as nucleation sites for the formation of slowly responding clusters. However, for the dielectric response, the average magnitude of polarization is not important; rather, the fluctuations around the average dipole moment play a key role. Thus it is possible for a Nb^{TM} site to exhibit a large local polarization and yet display very weak memory in its oscillations. In contrast, the Nb^{TT} sites, which may be only weakly polarized on average, exhibit strong memory in their oscillations around $P_i = 0$.

The slower relaxation observed at the Nb^{TT} sites is due to simple crystal chemical effects which lead to strong coupling between the displacements of Nb^{TT} and its Ti neighbors. Because O atoms between Nb and Ti are overbonded, the O-Nb and O-Ti bond lengths are strongly anticorrelated. With two such O neighbors, the Nb^{TT} atom must coordinate its oscillations with its two Ti neighbors, slowing down the Nb^{TT} dynamics. The hypothesis that slow relaxation times for $T < T_b$ are due to stronger coupling between the displacements of adjacent B cations is supported by the site-resolved real-space dipole-dipole correlation function $\Phi_i(r)$ [Fig. 3(b), inset]. At T_b a large number of sites exhibit fairly high $\Phi_i(r)$ values (between 0.08 and 0.1), and these are the same sites which have $\tau_i > 0.5$ ps. Above T_b only a small number of Nb^{TT} sites exhibit such high $\Phi_i(r)$ values, and they have a smaller τ_i. This shows that the dielectric response slows down when correlations are present for more than just a few Nb^{TT} sites.

The present work explains the recent phenomenological finding that the compositional phase transitions from regular ferroelectric to relaxor phase show a strong dependence on the second moment of oxygen B cation neighbor valence $\langle V^2 \rangle$ [17]. For a small number of overbonded oxygen atoms (corresponding to small values of $\langle V^2 \rangle$), extensive networks of correlated dipoles are never formed and the sites that have strong displacement coupling and high $\Phi_i(r)$ values remain isolated and uncoupled. For systems with a large number of overbonded oxygen atoms, dispersion increases.

In summary, our atomistic molecular dynamics simulations reproduce the essential features of the dielectric response of the classic PMN-PT relaxor system. This suggests that long-range chemical inhomogeneity and interactions between nanoscale polar regions are not necessary to give rise to the relaxor behavior. We show that local crystal chemistry is of crucial importance, with the presence of the overbonded oxygen atoms near the Nb^{TT} sites promoting the nucleation of networks of slowly responding dipoles, and the presence of underbonded oxygen atoms near the Nb^{MM} sites giving rise to fast relaxation (paraelectric matrix) even in the relaxor phase.

I. G. was supported by the Office of Naval Research Grant No. N00014-09-1-0157 and A. M. R. by the NSF MRSEC Program, Grant No. DMR05-20020. Computational support was provided by a Challenge Grant from the HPCMO of the U.S. Department of Defense, the Center for Piezoelectrics by Design, and the DURIP program.

[1] G. A. Smolenskii, V. A. Isupov, A. I. Agranovskaya, and S. N. Popov, Sov. Phys. Solid State **2**, 2584 (1961).
[2] I.-K. Jeong, T. Darling, J. K. Lee, T. Proffen, R. H. Heffner, J. S. Park, K. S. Hong, W. Dmowski, and T. Egami, Phys. Rev. Lett. **94**, 147602 (2005).
[3] R. Blinc, J. Dolinšek, A. Gregorovič, B. Zalar, C. Filipič, Z. Kutnjak, A. Levstik, and R. Pirc, Phys. Rev. Lett. **83**, 424 (1999).
[4] R. Blinc, V. Laguta, and B. Zalar, Phys. Rev. Lett. **91**, 247601 (2003).
[5] P. M. Gehring, S. E. Park, and G. Shirane, Phys. Rev. Lett. **84**, 5216 (2000).
[6] W. Dmowski, S. B. Vakhrushev, I.-K. Jeong, M. P. Hehlen, F. Trouw, and T. Egami, Phys. Rev. Lett. **100**, 137602 (2008).
[7] S. Tinte, B. P. Burton, E. Cockayne, and U. V. Waghmare, Phys. Rev. Lett. **97**, 137601 (2006).
[8] M. Roth, E. Mojaev, E. Dul'kin, P. Gemeiner, and B. Dkhil, Phys. Rev. Lett. **98**, 265701 (2007).
[9] S.-E. Park and T. R. Shrout, J. Appl. Phys. **82**, 1804 (1997).
[10] D. Viehland, S. J. Jang, L. E. Cross, and M. Wuttig, Phys. Rev. B **46**, 8003 (1992).
[11] R. Pirc, R. Blinc, and V. Bobnar, Phys. Rev. B **63**, 054203 (2001).
[12] V. Bovtun, S. Veljko, S. Kamba, J. Petzelt, S. Vakhrushev, Y. Yakymenko, K. Brinkman, and N. Setter, J. Eur. Ceram. Soc. **26**, 2867 (2006).
[13] G. Burns and F. H. Dacol, Solid State Commun. **48**, 853 (1983).
[14] V. Bobnar, Z. Kutnjak, R. Pirc, R. Blinc, and A. Levstik, Phys. Rev. Lett. **84**, 5892 (2000).
[15] M. A. Akbas and P. K. Davies, J. Am. Ceram. Soc. **80**, 2933 (1997).
[16] L. Farber and P. Davies, J. Am. Ceram. Soc. **86**, 1861 (2003).
[17] I. Grinberg, P. Juhas, P. K. Davies, and A. M. Rappe, Phys. Rev. Lett. **99**, 267603 (2007).
[18] See EPAPS Document No. E-PRLTAO-103-057943 for information about the parameters in the atomistic model used for the molecular dynamics simulations and the details of the molecular dynamics simulation procedure. For more information on EPAPS, see http://www.aip.org/pubservs/epaps.html.
[19] L. S. Kamzina, I. P. Raevskiĭ, S. M. Emel'yanov, S. I. Raevskaya, and E. V. Sahkar, Phys. Solid State **46**, 908 (2004).
[20] We define τ as the time at which $\Phi(t)$ reaches one tenth of its initial value.